Plant Cell Reports (2026) 45:117
https://doi.org/10.1007/s00299-026-03796-8

RESEARCH

Chromosome-level genome assembly, annotation, evolutionary analysis, and establishment of transformation systems in *Carex rigescens*

Luyu Wang[1] · Chengze Ma[1] · Yue Li[1] · Kai Zhu[1] · Chu Wang[1] · Yiming Wu[1] · Qiannan Hu[1] · Yan Sun[1]

Received: 6 January 2026 / Accepted: 25 March 2026 / Published online: 7 April 2026

Abstract

Key message **Using PacBio and Hi-C technologies, we generated a chromosome-level whole-genome assembly of *Carex rigescens* and established its genetic transformation system, which provides novel insights into the research of this species.**

Abstract *Carex rigescens* is an important turfgrass species and grass for ecological restoration, but the lack of genomic resources in the genus Carex has hindered its genetic improvement. In this study, *C. rigescens* was determined to be diploid (2n = 60) by flow cytometry and chromosome visualization. We generated a high-quality genome assembly of *C. rigescens* via a combination of Illumina, PacBio, and Hi-C technologies, with 300 Mb of sequences anchored to 30 chromosomes. This genome contains 59,761 functionally annotated protein-coding genes (91.28%), and repetitive sequences account for 33.28% of the total genome length. Evolutionary analysis reveals that one WGD event had occurred in *C. rigescens* and that an LTR burst in *C. rigescens* occurred around 0.04 Mya. We also performed WOX gene family analysis, including its localization and classification on the chromosomes of *C. rigescens*, as well as the analysis of cis-acting elements in the *CrWOX14* promoter. The first efficient regeneration and transformation system was established. These findings provide new insights into the characterization and evolution of the genomes of the genus *Carex* and provide a reference for comparative genetic and genomic studies of the genus *Carex*. They also lay the foundation for the acquisition of transgenic *C. rigescens*.

Keywords *Carex rigescens* · Genome sequence · WOX transcriptional factors · Regeneration and transformation system

Introduction

The genus Carex L. is a monoecious, self-pollinated, perennial herb of the Cyperaceae family (Friedman and Barrett 2009). It has a wide distribution range, with about 2,000 species in the world and nearly 500 species in China, and is one of the largest genera in the Cyperaceae family (Schütz 2000). *Carex rigescens* (Franch.) V. Krecz is a perennial plant of

Communicated by H Shi.

Luyu Wang and Chengze Ma contributed equally to this work.

✉ Qiannan Hu
qnanhu@cau.edu.cn

✉ Yan Sun
02008@cau.edu.cn

Luyu Wang
b20243010024@cau.edu.cn

Chengze Ma
mczturf@cau.edu.cn

Yue Li
liyue2020@cau.edu.cn

Kai Zhu
zhukai@alu.cau.edu.cn

Chu Wang
bs20223241083@cau.edu.cn

Yiming Wu
20223243495@cau.edu.cn

[1] Department of Turfgrass Science and Engineering, College of Grassland Science and Technology, China Agricultural University, Beijing 100193, People's Republic of China

the genus *Carex*, widely distributed in northern China. *C. rigescens* has high garden value due to its early rejuvenation, green slender leaves, neat appearance, good coverage, well-developed root system, fast growth, and wide distribution. When used as a lawn grass species, it can be used as a single lawn grass species or mixed with other grass species to form a composite lawn (Wan 2001). It can be adapted to a variety of soil conditions and is commonly used in urban and rural general greening, road slope greening, and ecological restoration with grass species. It is expected to play a huge role in lakeshore landscaping, water purification, soil and water conservation, as well as embankment greening (Oprea et al. 2022).

C. rigescens has long adapted to intrinsic reproductive strategies, with vegetative propagation becoming its dominant reproductive mode and seed reproduction being nearly lost (Schütz and Milberg 1997; Schütz 1998). Its seeds are deeply dormant and germination rates are generally low (Schütz 1997). At the same time, the ploidy and chromosome number of *C. rigescens* are not clear, genomics research is lagging behind, and the genome sequence and structure information is almost blank. Traditional breeding methods are long and very restrictive. Plant genetic transformation is an important technological advance in modern science that has not only contributed to fundamental insights into plant biology, but also ushered in a new era of plant improvement and commercial agriculture (Su et al. 2023). For most turfgrass species, efficient genetic transformation and regeneration remain a major challenge due to strong genotype dependence and limited availability of suitable explants, even after decades of technological advances in this field (Lee 1996; Longo et al. 2006). Rogers used seedlings germinated from *C. lurida* to induce callus tissue, but the buds could not regenerate from the callus tissue, and the callus tissue eventually turned black (Rogers 2003). There is currently no genetic transformation system for *C. rigescens*, which hinders the development and utilization of this genus, the improvement of varieties, and enhancement of the seed propagation capacity. Therefore, it is necessary to establish an efficient regeneration and transformation system. Previous studies have shown that members of the WOX family have multifunctional transcription factors involved in plant growth and development throughout the plant life cycle, from meristematic tissue maintenance to embryonic pattern (Hao et al. 2019; Jha et al. 2020; Fambrini et al. 2022). Although WOX transcription factors are recognized as developmental regulators, studies have also shown that WOXs are involved in some abiotic stress responses (Tang et al. 2020; Chen et al. 2024). Gene family analysis remains difficult in the absence of a reference genome at this time.

In this study, we used a combination of Illumina, PacBio, and Hi-C technologies to perform a comprehensive assembly of the *C. rigescens* genome to understand its genomic features and evolution. We also performed gene family analysis of the *C. rigescens* WOX family and established the first efficient regeneration and transformation system for *C. rigescens*. Our results provide an important genomic resource for the field of *Carex* genus biology and genetic improvement and contribute to the development of transgenic *C. rigescens* species. The WOX family provides a rich resource for further study of *CrWOX* transcription factors in *C. rigescens*.

Materials and methods

Ploidy analysis

C. rigescens material used for sequencing was obtained from the China Agricultural University Shangzhuang Experimental Station (40。13’ N, 116。18’ E) in Beijing, China. To obtain mitotic metaphase chromosomes with well-defined morphological features, the meristematic regions of *C. rigescens* root tips (with active mitotic division) were digested with Cellulase R-10 and Pectinase Y-23 (Yakult) (Cao et al. 2023). The chromosome images were captured with a DP70 CCD under an Olympus BX53 fluorescence microscope with DAPI. The images were processed by Adobe Photoshop 2020. The ploidy of *C. rigescens* was also determined by flow cytometry and the diploid *Carex breviculmis* material was used as a reference (Galbraith et al. 2001).

Genome sequencing

We used a modified CTAB method to extract leaf DNA from *C. rigescens* and determined the concentration and quality of the extracted *C. rigescens* DNA by agarose gel electrophoresis and a NanoDrop 2000 spectrophotometer (Stacey and Isaac 1994). For Illumina library preparation and sequencing, we first fragmented qualified genomic DNA into 350 bp fragments via ultrasonication. Subsequently, short-read sequencing libraries were constructed using the VAHTSTM Fg DNA Library Prep Kit for Illumina (Cat. No. ND617-02), following end repair, A-tailing, adapter ligation, target fragment selection, and PCR amplification. Library fragment size and concentration were assessed using Qseq400 and Qubit systems to verify compliance with sequencing standards. The library was immobilized onto sequencing chips via bridge PCR. Paired-end 150 bp (PE 150) sequencing was performed on an Illumina NovaSeq platform using the NovaSeq TM X Series 25B Rgt Kit (Cat. No. 20104706). The resulting sequencing data were subjected to quality control prior to subsequent bioinformatic analysis. The short reads from Illumina platform were quality filtered by fastp (Chen et al. 2018) using the parameters -q 10 -u 50 -y -g -Y 10 -e 20 -l 100 -b 150 -B 150. The quality filtered reads were used for genome size estimation. We counted the 18-kmers

with Jellyfish (Marçais and Kingsford 2011) software and calculated the genome characteristics using GenomeScope (Ranallo-Benavidez et al. 2020) software.

To construct libraries for PacBio sequencing, high-quality genomic DNA was extracted first and then subjected to fragmentation with a g-TUBE instrument (Covaris). Following fragmentation, DNA products were subjected to purification and recovery using AMPure PB magnetic beads. Subsequently, the concentration of the recovered products was quantified with a Qubit fluorometer, and their size distribution was evaluated via an Agilent 2100 Bioanalyzer. A total of 5 μg of fragmented DNA was subjected to damage repair, end repair, and adapter ligation using the SMRTbell Template Prep Kit (Pacific Biosciences). Subsequently, the adapter-ligated products were subjected to size selection via the BluePippin Size-Selection System, and the target fragments were purified and recovered using AMPure PB magnetic beads. To eliminate potential DNA damage induced during size selection, the gel-extracted products underwent a second round of damage repair with the SMRTbell Damage Repair Kit (Pacific Biosciences), followed by another purification step using AMPure PB magnetic beads. The final library (post-secondary damage repair) was characterized by concentration quantification using a Qubit fluorometer and size distribution analysis via an Agilent 2100 Bioanalyzer to verify compliance with on-machine sequencing requirements. Prior to sequencing, the qualified library was subjected to primer and polymerase binding using the PacBio DNA/Polymerase Kit: specifically, Primer V2 and Polymerase P6 were used for the RSII platform, while Primer V3 and Polymerase 2.0 were adopted for the Sequel platform. The resulting reaction products were further bound to sequencing-grade Magbeads. Finally, the Magbead-bound library was loaded onto a Sequel II sequencer for PacBio sequencing. We ultimately obtained 16.06 Gb of clean data, with a read N50 of 19.41 kb and an average read length of 18.67 kb. Clean data refers to high-confidence sequencing reads obtained by applying a series of quality filtering and redundancy removal steps to raw sequencing data (raw reads). These reads are used for subsequent genome assembly or analysis, involving the removal of adapter contamination sequences, filtering of low-quality reads, elimination of redundant or anomalous reads, and exclusion of organelle DNA contamination.

Genome assembly

A genome assembly was generated from high-accuracy HiFi reads using hifiasm v0.19 (Cheng et al. 2021). Haplotype-specific error correction was then performed, in which all HiFi reads were loaded into memory for all-vs-all alignment and subsequent error correction. Sequencing errors were corrected based on nucleotide information supported by at least three reads. Simultaneously, homozygous data were utilized for error correction, while heterozygous variants were preserved and SNP phasing was completed. Subsequently, a phased string-graph was constructed based on retained heterozygous information. This assembly graph, with reads as vertices and overlapping regions as edges, fully preserves all bubble structures and retains genome-wide haplotype information. During assembly, primary contigs are randomly selected from one side of each bubble. The final combination chosen uses a '-n' parameter of 4 (removing unitigs with fewer than 4 supporting reads) and a '-l' parameter of 2 (splitting haplotypes to yield a single-genome size). This approach yields an assembly size close to the reference single genome (307,028, 497 bp) and a Contig N50 of 2,938,588.

For anchored contigs, 178,972,551 clean read pairs were generated from the Hi-C library and mapped to the polished *C. rigescens* genome using BWA (bwa-0.7.17) with the default parameters (Rao et al. 2014). Paired reads with mate mapped to a different contigs were used for Hi-C-associated scaffolding. Self-ligation, non-ligation, and other invalid reads, such as Start NearRsite, PCR amplification, random breaks, large small fragments, and extreme fragments, were filtered. We then successfully clustered 2799 contigs into 30 groups with the agglomerative hierarchical clustering method in Lachesis (Burton et al. 2013). Lachesis was further applied to order and orient the clustered contigs. A total of 1410 contigs were successfully ordered and oriented, with a total length of 629,439,453 bp. Finally, we obtained the first chromosome-level high-quality assembly, with chromosomal lengths from 5.562 Mb to 16.414 Mb, containing 96.18% of the total sequence.

Genome quality evaluation

The mass-filtered reads were used to estimate genome size. The K-mer frequency distribution was counted by Jellyfish (Marçais and Kingsford 2011) (2.1.4 https://github.com/gmarcais/Jellyfish) in 21-kmers and the genome characterization was calculated by GenomeScope (Ranallo-Benavidez et al. 2020) (v 2.00) (https://github.com/tbenavi1/genomescope2.0). Several large evolutionary branches of single-copy genomes were constructed from the embryophyte database of the direct homology database OrthoDB 10 (http://cegg.unige.ch/orthodb). The genome was aligned with the assembled genome and evaluated according to the ratio and completeness of the alignment using BUSCO v5.2.1 (Benchmarking of Universal Single-Copy Homologs) (Simão et al. 2015). Integrity and uniformity of sequencing coverage of assembled genomes from second-generation versus HiFi reads sequencing were assessed using bwa (v0.7.17-r1188) and Minimap2, respectively.

Filtering of Hi-C data and evaluation of sequencing data utilization were done by HiC-Pro (v2.10.0), and comparison of sequenced bipartite data with assembled genome sequences was done by bwa (v 0.7.17-r1188; comparison mode: aln;) (Li and Durbin 2009). For quality assessment of the Hi-C assembly, the genome of the anchor allele of the Hi-C assembly was isometrically sheared into 300,000 bp partitions and the number of Hi-C read pairs in any two intervals was used as a signal for the strength of the interaction between the two partitions.

Genome annotation

To complete genome annotation, coding genes and non-coding RNAs were predicted and evaluated, while repetitive sequences, gene functions, and pseudogenes were annotated. Annotation of repetitive sequences was performed using an integrated computational pipeline. Transposable elements (TEs) and tandem repeats were annotated separately as detailed below. TEs were identified by a combination of homology-based and de novo approaches. We first constructed a de novo repeat library for the genome using RepeatModeler (http://www.repeatmasker.org/RepeatModeler/) (Flynn et al. 2020), which automatically integrates two de novo repeat detection programs, RECON and RepeatScout. Full-length long terminal repeat retrotransposons (fl-LTR-RTs) were identified using LTRharvest (v1.5.9) and LTR_finder (v2.8), and high-quality, non-redundant intact fl-LTR-RTs were further generated using LTR_retriever (Ou and Jiang 2018). A non-redundant, species-specific TE library was then constructed by combining the de novo TE library with the known Dfam (v3.5) database. Finally, TEs in the *C. rigescens* genome were identified and classified via homology search against this library using RepeatMasker (v4.12) (Tarailo-Graovac and Chen 2009). Tandem repeats were annotated using the Tandem Repeats Finder (TRF 409) (Benson 1999) and MIcroSAtellite identification tool (MISA v2.1) (Beier et al. 2017).

Annotation of protein-coding genes was performed by integrating three complementary strategies, namely de novo prediction, homology-based search, and transcript-based assembly. De novo gene models were predicted using two ab initio gene-prediction tools: Augustus (v3.1.0) (Stanke et al. 2008) and SNAP (2006–07-28) (Korf 2004). For the homology-based approach, gene models were predicted with GeMoMa (v1.7) (Keilwagen et al. 2016) using reference gene models from closely related species in the *C. rigescens* lineage. For the transcript-based prediction, RNA-sequencing reads were mapped to the assembled genome using Hisat2 (v2.1.0) (Kim et al. 2015) and assembled using StringTie (v2.1.4) (Pertea et al. 2015), and GeneMarkS-T (v5.1) was applied to predict gene structures from the assembled transcripts (Tang et al. 2015). PASA (v2.4.1) (Haas et al. 2003) was used to generate gene models based on unigenes and full-length transcripts from PacBio or ONT sequencing assembled by Trinity (v2.11). Gene models predicted by the above methods were combined and integrated using EVM (v1.1.1) (Haas et al. 2008), followed by further refinement and update with PASA. Functional annotation of protein-coding genes was performed by aligning gene sequences against multiple public databases, including the National Center for Biotechnology Information (NCBI) (https://www.ncbi.nlm.nih.gov/) Non-Redundant (NR) (202,009,ftp://ftp.ncbi.nlm.nih.gov/blast/db), EggNOG (http://eggnog5.embl.de/download/ eggnog_5.0/), KOG, TrEMBL, Swiss-Prot, and Kyoto Encyclopedia of Genes and Genomes (KEGG) (http://www.genome.jp/kegg/) databases, using diamond blastp (v0.9.29.130) with an E-value threshold of 1E-3. Protein domains were annotated using InterProScan (v5.34–73.0) based on the InterPro database, and conserved motifs and domains were further identified against the Pfam database. Gene Ontology (GO) IDs for each gene were assigned based on annotations from TrEMBL, InterPro, and EggNOG.

Annotation of non-coding RNA genes was performed using multiple bioinformatics tools. Transfer RNA (tRNA) genes were identified using tRNAscan-SE (v1.3.1) (Lowe and Eddy 1997) with default parameters. Ribosomal RNA (rRNA) genes were predicted using barrnap (v0.9) with default parameters. MicroRNAs (miRNAs), small nuclear RNAs (snRNAs), and small nucleolar RNAs (snoRNAs) were identified by searching against the Rfam (v14.5) (Griffiths-Jones et al. 2005) database using Infernal (v1.1) (Nawrocki and Eddy 2013) with default parameters. Pseudogene prediction was conducted to identify non-functional gene copies derived from functional genes. Pseudogenes typically share high sequence similarity with functional genes but have lost their biological functions due to genetic mutations, including insertions and deletions. The GenBlastA (v1.0.4) program was used to scan the entire genome after masking the predicted functional genes. Putative pseudogene candidates were then verified by detecting premature stop codons and frame-shift mutations using GeneWise (v2.4.1) (She et al. 2009).

Evolutionary analysis

Comparison of protein sequences from ten species (*O. sativa*、*J. inflexus*、*J. effus*、*C. scoparia*、*C. rigescens*、*C. littledalei*、*C. cristatella*、*B. distachyon*、*A. trichopoda*、*A. thaliana*) was performed using OrthoFinder (v2.4.0) (Emms and Kelly 2019). The obtained gene families were annotated using the Pfam V33.1 database (Mistry et al. 2021). Protein sequences of single-copy homologous genes were aligned using mafft (v7.205) (Katoh et al. 2009) and phylogenetic trees were constructed using iqtree (v2.2.0)

(Nguyen et al. 2015). Gene family expansions and contractions were analyzed using CAFE (v4.2) (Han et al. 2013), and KEGG pathways were analyzed for functional enrichment using the R package (https://github.com/StoreyLab/qvalue) to adjust *p*-values. WGD events were recognized using wgd (v3.7.3) (Zwaenepoel and Peer 2019) and custom scripts (https://github.com/JinfengChen/Scripts).

The fl-LTR-RTs were characterized using LTRharvest (v1.5.10) (Ellinghaus et al. 2008) and LTR_finder (v1.07) (Xu and Wang 2007). LTR_retriever was then used to generate high-quality complete fl-LTR-RT and non-redundant LTR libraries (Ou and Jiang 2018). Flanking sequences on both sides of the LTR were extracted, compared with mafft (v7.205) (Katoh et al. 2009), and distances were calculated using the Kimura model in EMBOSS (v6.6.0) (Rice et al. 2000). Genetic covariance analysis was performed using diamond v0.9.29.130 (Buchfink et al. 2015) to compare the genetic sequences of the two species and identify pairs of similar genes (e < 1e-5, C score > 0.5, where C score values were filtered using JCVI). mCScanX (parameter-m 15) was used to determine whether similar gene pairs were chromosomally close to each other based on gff3 files (Wang et al. 2012).

Gene family analysis

WOX protein sequences from *Arabidopsis thaliana*, *Oryza sativa*, and *Brachypodium distachyon* were downloaded from PlantRegMap (https://plantregmap.gao-lab.org/index.php, accessed April 1, 2024), and localized BLASTp searches were performed with the *C. rigescens* whole protein sequence database using Tbtools (e values ≤ e-10) (Chen et al. 2023). Then all sequences were searched at Interpro (https://www.ebi.ac.uk/interpro/, accessed April 1, 2024) for the presence of the PF00046 structural domain. All WOX genes were finally identified in *C. rigescens*. For chromosomal location and synteny analysis of CrWOXs, chromosomal position information of WOX transcription factors was extracted based on the annotated gff3 file of *C. rigescens* and visualized using Tbtools (Chen et al. 2023). Intraspecific co-lineage relationships of the WOX gene family were analyzed using the MCScanX (Wang et al. 2012). For phylogenetic analysis, amino acid sequences of the WOX family among *Arabidopsis thaliana*, *Oryza sativa*, *Brachypodium distachyon,* and *C. rigescens* were compared using ClustalW in MEGA with the maximum-likelihood (ML) method (Tamura et al. 2021). For gene structure and cis-acting element analysis, gene structures were analyzed and visualized according to genome sequences using TBtools and 2000 bp upstream of the ATG of the *CrWOXs* gene was extracted for promoter analysis.

Cis-acting elements in the 2 kb promoter region upstream of the *C. rigescens* WOXs gene family were identified on the PlantCARE website (https://bioinformatics.psb.ugent.be/webtools/plantcare/html/, accessed April 1, 2024) (Lescot et al. 2002) and visualized using Microsoft Excel 2010.

Embryogenic callus induction and regeneration

The seeds of *Carex rigescens* were used as explants to induce embryogenic callus. For surface sterilization, seeds were soaked in 20% (w/v) sodium hypochlorite (NaClO) for 40 min and rinsed eight times with sterile distilled water. After drying, the seeds were placed on solid callus induction medium (MS2) based on MS basal medium (Owen et al. 1991) supplemented with 2 mg/L 2,4-D, 1 mg/L 6-BA, 1 mg/L NAA, 30 g/L sucrose, and 3 g/L gel (pH 5.95). We also tested other hormone-containing combinations in the culture medium (Table S2). After 6–8 weeks in the dark incubator at 25 °C, embryogenic callus tissue of *C. rigescens* was picked out and transferred onto the fresh MS induction medium for propagation every 4 weeks. After subculturing three to five times, the callus was transferred to regeneration medium (MG) based on MS basal medium supplemented with 1 mg/L 6-BA and 0.01 g/L Tdz for developing buds. Then the regenerated shoots were transferred to 1/2MS medium for developing roots. Regeneration was carried out in a growth chamber at 25 ℃ under a 16-h photoperiod with a light intensity of 200 μmol m^{-2} s^{-1}.

Agrobacterium-mediated transformation

The binary vector pGFPGUSPlus (Vickers et al. 2007) was used for establishing an *Agrobacterium*-mediated transformation. The vector carries the HygB gene as a selection marker and GUS as a reporter gene in its T-DNA region, both under the control of the 35S promoter. *A. tumefaciens* strain EHA105 was inoculated into liquid YEP medium with continuous shaking until its OD_{600} reached 0.8 (Table S3). Small pieces of embryogenic calli (0.5–1.0 mm in diameter) were immersed in the *Agrobacterium* culture for 30 min at room temperature. Vacuum infiltration was then performed for 10 min, after which the callus pieces were transferred onto sterile filter paper to remove excess bacterial suspension. The calli were transferred onto callus selection medium containing MS2 supplemented with 200 mg/L HygB and 200 mg/L cefotaxime. The calli were incubated at 28 °C for selection and subcultured every 4 weeks. After 10–12 weeks of selection, HygB-resistant calli were transferred to MG and 1/2MS supplemented with 100 mg/L HygB and 100 mg/L cefotaxime for regeneration.

GUS assay and PCR analysis

GUS activity was examined histochemically by staining callus or leaf fragment excised from putative transgenic plants

in GUS staining solution (Ren et al. 2005). Tissues were incubated overnight at 37 °C in a phosphate-buffered solution containing 1 mg/mL X-Gluc. Genomic DNA was isolated from approximately 0.5 g of leaves using the CTAB method. PCR reaction solution (20 µL) consisted of DNA sample (20 µg), forward primer NPT-F (5′-GCATATCAA TAAGCGGAGGAAAAG-3′) (10 µM), reverse primer NPT-R (5′-GGTCCGTGTTTCAAGACGG-3′) (10 µM), and Taq DNA polymerase (0.5 U).

Results

Genome sequencing and assembly

Carex rigescens (Franch.) V. Krecz is a perennial herb of the genus *Carex* (Cyperaceae) that is widely distributed in northern China, including Liaoning, Hebei, Henan, and Shandong provinces and the Inner Mongolia Autonomous Region (Fig. 1A) (Hu et al. 2021). We found 30 pairs of chromosomes in a mid-mitotic division root somatic cell (Fig. 1B) and that *C. rigescens* was diploid, as measured by FISH and flow cytometry using diploid *Carex breviculmis* as a reference (Fig. 1C, D) (Jia et al., 2024). Flow cytometry analysis showed that the mean fluorescence intensity of *Carex breviculmis* in nuclei was 627.67 (CV = 4.57%). In comparison, *Carex rigescens* exhibited a mean fluorescence intensity of 807.19 (CV = 4.00%). DNA from fresh leaves of *C. rigescens* was isolated and sequenced. Illumina sequencing produced approximately 28.87 Gb of short reads (Table S4). The K-mer frequency distribution (k-mer = 21) plots estimated that the genome size was about 307.03 Mb and the genome heterozygosity was 2.41% (Figure S2). Therefore, the genome of *C. rigescens* is a complex genome with high heterozygosity.

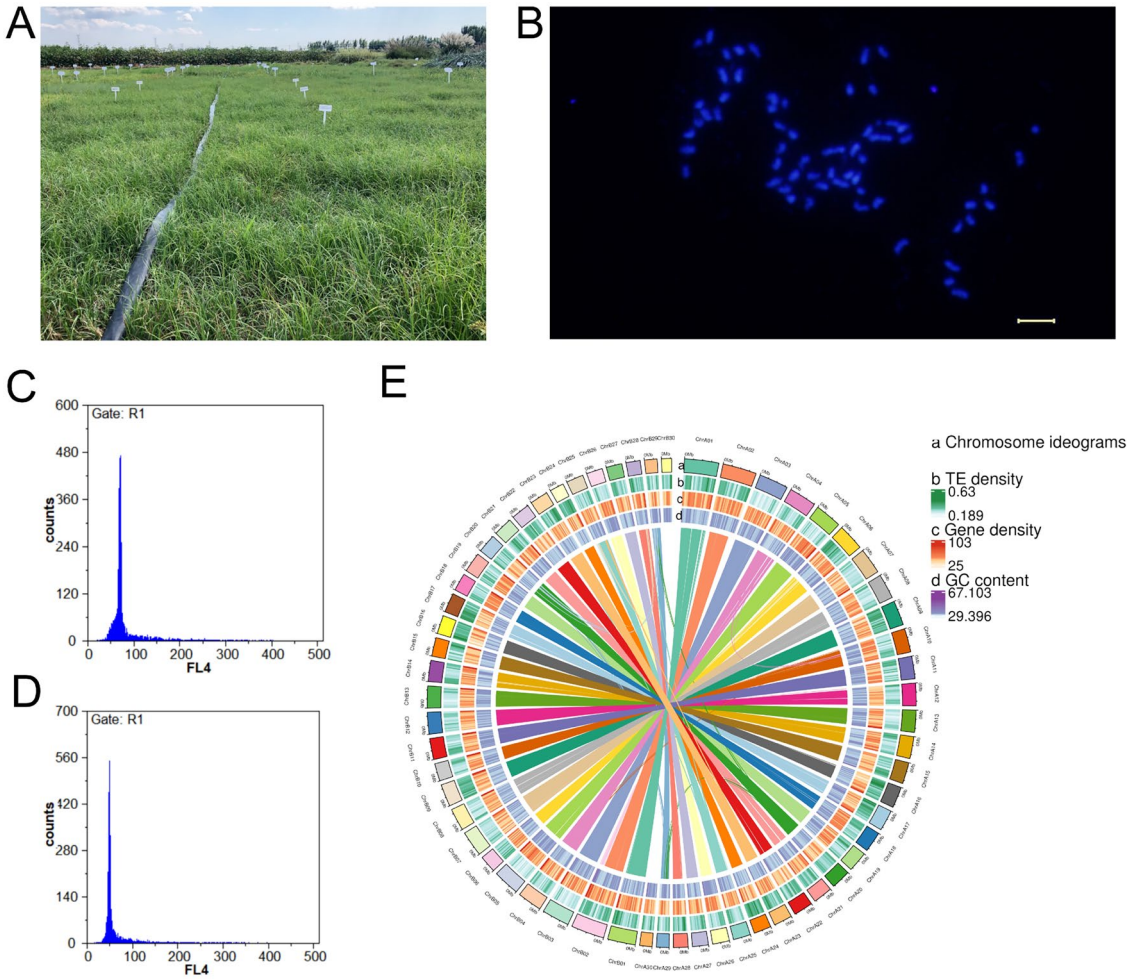

Fig. 1 Ploidy characteristics of *Carex rigescens*. **A** *Carex rigescens* lawn. **B** Mitotic metaphase chromosome visualization. **C** Flow cytometric analysis results of *Carex rigescens.* **D** Flow cytometric analysis results of *Carex breviculmis* -treated group. **E** Circos plot showing the genome characteristics

For accurate assembly in this highly heterozygous plant, we sequenced the genome by utilizing a combination of Illumina, Pacbio, and Hi-C approaches, and assembled the sequences by using a series of methods. Pacbio sequencing produced approximately 16.06 Gb of long reads and Hi-C sequencing produced 53.44 Gb of high-quality clean reads (Table S4). Among the four parameter combinations tested for hifiasm assembly, the combination with i = 2 and *n* = 4 yielded the optimal genome assembly (Table 1). The BUSCO indicated that 93.43% of the core eukaryotic genes consisted of 140 single-copy orthologs and 1376 duplicated orthologs (Table S5). To evaluate the integrity of the assembly and the uniformity of sequencing coverage, the assembled genome was also aligned with short reads and HiFi reads. The comparison rates 96.74% and 99.70% indicate a complete genome assembly.

We ultimately assembled two haplotypes, measuring 300.74 Mb and 281.64 Mb, respectively, which closely matched the K-mer results (Table S11). The final chromosome-level genome assembly of *C. rigescens* is 300.74 Mb in size and composed of 2799 contigs with a contig N50 of 2.94 Mb and a scaffold N50 of 9.46 Mb (Table 1). After Hi-C assembly, genome sequences were mapped on 30 chromosomes, accounting for 92.53% (Fig. 1E). Among the sequences mapped to chromosomes, those for which the order and orientation could be determined were 289.25 Mb in length, accounting for 96.18% of the total length of the localized chromosome sequences. Similarly, strong Hi-C signals between each chromosome pair among 30 chromosomes showed that the interaction intensity between adjacent sequences (diagonal position) was high, while the interaction signal strength between non-adjacent sequences (non-diagonal position) was weak. This is consistent with the principle of Hi-C genome assembly, which proves high-quality genome assembly with accurately phased chromosomes (Figure S3). For Hi-C data quality assessment, we used HiCUP v0.9.2 to evaluate key metrics. The ratio of short-range cis contacts (< 10 kbp) to long-range cis contacts (> 10 kbp) was 0.219, and the cis/trans interaction ratio was 0.309. These values reflect species-specific chromosomal architecture, with a relatively high proportion of trans-chromosomal contacts compared to human (53.9%), fruit fly (21.1%), and yeast (15.1%) (Wingett et al. 2015). To assess potential cross-species contamination, 10,000 clean reads were randomly sampled and aligned to the NCBI NT database using BLAST v2.2.31. The top five matching species all belonged to the genus "*Carex*", confirming no significant exogenous contamination (Table S1).

Table 1 Statistics of the sequencing and assembly of the *Carex rigescens* genome

Chromosome number	2n = 2x = 60	
Illumina sequencing	Clean data size	28.87 Gb
	Estimation of genome size	307.03 Mb
	The content of repeats	33.28%
Pacbio sequencing	Clean data size	16.06 Gb
Hifi assembly	Total number of contigs	2799
	Contig N50	2,938,588
	Contig N90	89,335
Hi-C sequencing	Clean data size	53.44 Gb
Scaffolds assembly	Assembled genome size	300.74 Mb
	Total number of scaffolds	1023
	Chromosome-anchored%	92.53%
	The length of scaffolds N50	9,456,327
	The length of scaffolds N90	534,520
	The content of GC	34.05%

Genome annotation

Protein-coding genes were annotated according to a combination of ab initio, homology, and transcriptome analysis methods (Table 2). We predicted a total of 59,761 genes, with an average gene length of 3275.75 bp, 309,151 CDS, and an exon number of 317,238. 95.35% of BUSCO genes were present in our predicted genes, indicating high completeness of gene prediction (Table S5). In addition, 1,510 tRNAs, 2,123 rRNAs, and 182 miRNAs were detected. A pseudogene is a gene that has a sequence similar to that of a functional gene but has lost its original function due to mutations such as insertions and deletions (Yadav et al. 2023). There were 204 pseudogenes predicted in our study. Through RepeatMasker prediction, we finally obtained a transposable element (TE) sequence of about 190,738,885 bp, accounting for 30.30% (Table 2; Table S7).

The predicted gene sequences were analyzed for annotation in the databases NR, eggNOG, GO, KEGG, TrEMBL, KOG, SWISS-PROT, and Pfam. A total of 91.28% of the genes could be annotated to the databases (Table S8). In

Table 2 Annotation of the *Carex rigescens* genome assembly

	Number	Length (bp)	Percentage
GC content			33.42%
Total TE sequences	765,028	190,738,885 bp	30.30%
Total tandem repeats	591,927	46,221,226 bp	7.34%
Coding genes	59,761	195,762,223 bp	
Average CDS	5.17	1208.23 bp	
Average exons per gene	5.31	1,479 bp	
Average length per intron	4.31	1706.75 bp	
Non-coding RNAs	4031		
Pseudogene	204	490,683 bp	
Motif	2,155		
Domain	57,430		

the KOG analysis, general function prediction was feasible for 29,153 genes. Of these, 7752 genes were associated with signal transduction mechanisms (Figure S4). In the GO annotation, 46,156 annotated genes were divided into the GO terms of biological process, cellular component, and molecular function, respectively.

Genome evolution

The genome evolution of *C. rigescens* was inferred based on single-copy orthologous genes of *O. sativa*, *J. inflexus*, *J. effusus*, *C. scoparia*, *C. littledalei*, *C. cristatella*, *B. distachyon*, *A. trichopoda*, and *A. thaliana*. Comparative genome analysis identified a total of 40,359 gene families (Table S9), of which 3124 were shared among the 10 plant species analyzed and 1505 were unique to *C. rigescens* (Fig. 2A). Among the 1505 gene families unique to *C. rigescens*, those involved in RNA polymerase were significantly enriched. The phylogenetic tree was constructed using 103 single-copy gene sequences (Figure S5), and the results indicated that *C. rigescens* was evolutionarily closer to *C. scoparia* and *C. cristatella*. The estimated time of divergence was approximately 8.42 million years ago (Mya). Further gene family analysis revealed that 1,908 gene families expanded, while only 2 contracted in the *C. rigescens* genome (Fig. 2B). Those involved in photosynthesis and flavonoid biosynthesis were significantly enriched in expanded gene families.

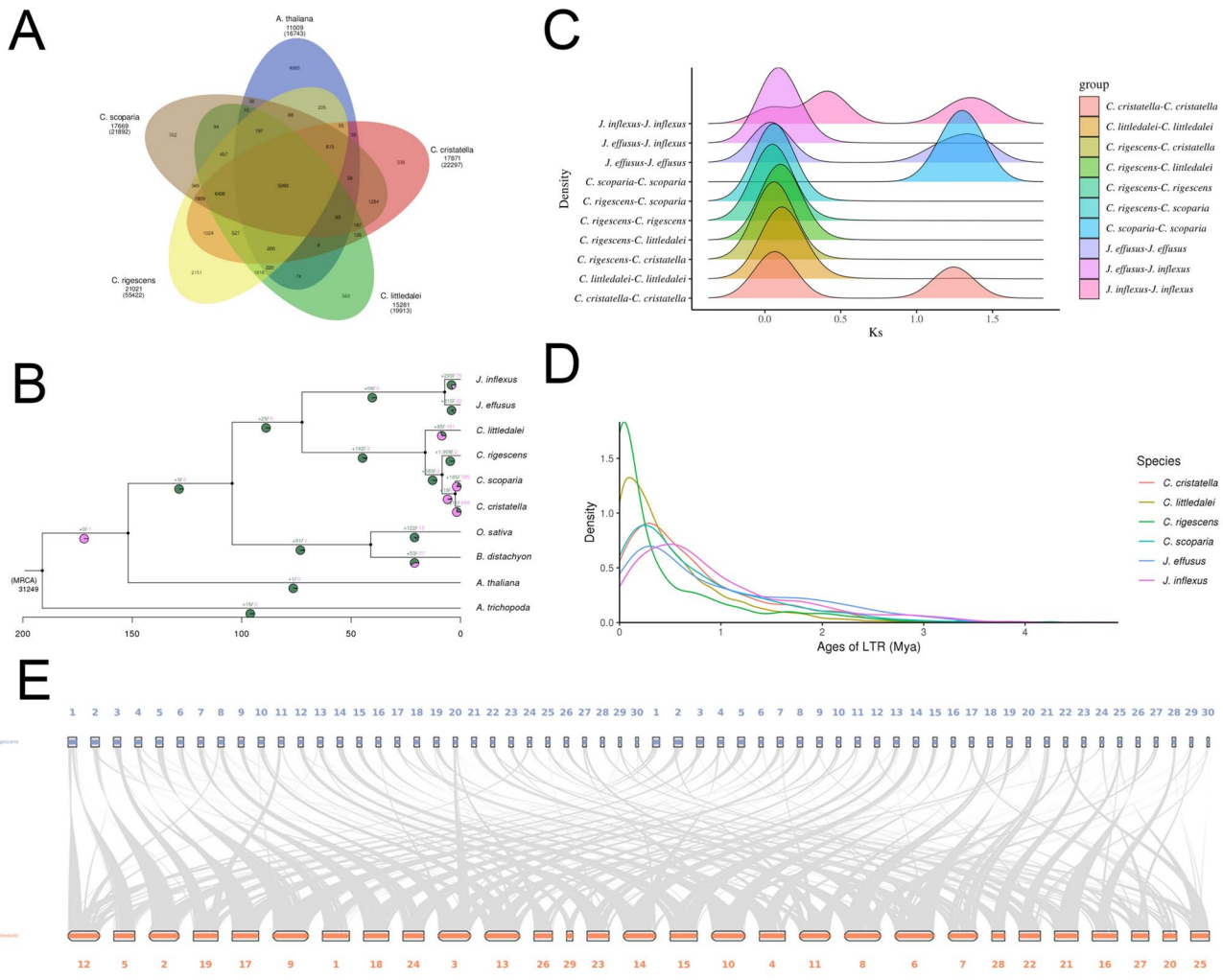

Fig. 2 **A** Venn diagram representing the distribution of shared gene families among *C. rigescens* and four other plants (*C. scoparia, C. littledalei, C. cristatella* and *A. thaliana*). **B** Phylogenetic tree showing gene family expansion/contraction analysis of *C. rigescens* and selected nine other plants. Numbers in green indicate expanded gene families, and numbers in purple indicate contracted gene families. **C** Representation of whole-genome duplication (WGD) events during the evolution of *C. rigescens* and nine other plants based on synonymous substitution rates (Ks). **D** Depiction of LTR evolution. **E** Macrosynteny analysis between the *C. rigescens* (2n) and *C. littledalei* (2n) chromosomes

Whole-genome duplication (WGD), also known as ancient polyploidization, is a process in which the entire genome is duplicated and doubled. It is important for the origin of species and the expansion of the genome (Qiao et al. 2022). To elucidate the polyploidy history of *C. rigescens* and related species, we examined the *K*s distributions of the paralogs and orthologs identified from *C. rigescens*, *C. scoparia*, *C. littledalei, and C. cristatella* (Fig. 2C). The major peaks in the Ks distribution of orthologs between *C. rigescens–C. scoparia* (0.27), *C. rigescens–C. littledalei* (0.43), and *C. rigescens–C. cristatella* (0.29) were all younger than *C. rigescens–C. rigescens* (3.17), *C. scoparia–C. scoparia* (4.53), *C. littledalei–C. littledalei* (4.02), *and C. cristatella–C. cristatella* (4.27), respectively. Therefore, we speculated that a shared WGD event had occurred in the common ancestor of *C. rigescens*, *C. scoparia*, *C. littledalei,* and *C. cristatella*, and that two independent WGD events had occurred in *C. cristatella*, which was consistent with a previous report (Planta et al. 2022).

Transposable element burst, along with climate events, may induce new speciation events due to rapid genetic variation. We found that the LTR burst in *C. rigescens* occurred around 0.04 Mya (Fig. 2D) and relatively close to *C. littledalei,* whose LTR burst occurred around 0.09 Mya. Genomic comparisons of *C. rigescens* and *C. littledalei* showed a high degree of genomic covariance. For example, *C. rigescens* chromosome 2 is highly collinear with *C. littledalei* chromosome 2 (Fig. 2E). Numerous chromosomal arms of *C. littledalei* were shuffled and duplicated within the *C. rigescens* genome. For example, the second largest chromosome in *C. rigescens* is merged by chromosome 12 and chromosome 5 in *C. littledalei*.

WOX gene family analysis

WOX plays an important role in plant development as a key transcription factor affecting regeneration efficiency and response to abiotic stress (Willoughby and Nimchuk 2021). Overexpression of the *TaWOX5* gene dramatically increases transformation efficiency with less genotype dependency in wheat (*Triticum aestivum* L.) (Wang et al. 2022b). *PagWOX11/12a* improves salt tolerance via ROS scavenging (Wang et al. 2021). To investigate the function of WOX in *C. rigescens, we* first predicted WOX transcription factors in the *C. rigescens* genome in PlantRegMap (https://plantregmap.gao-lab.org/index.php) and identified a total of 25 predicted WOX genes (Table S10), which were analyzed in Interpro to have conserved structural domains of the WOX family (PF00046). To further determine the evolutionary relationships of CrWOXs, we localized their positions on the chromosomes (Fig. 3A). Among them, WOX was most abundantly distributed on chromosome A10, and we also found three possible WOX. In addition, we constructed phylogenetic trees for WOXs in *Arabidopsis thaliana*, *Oryza sativa*, *Brachypodium distachyon,* and *C. rigescens*. The results showed that these WOXs can be categorized into three main groups, with most proteins in the WUS branch (Fig. 3B). For the gene structure analysis of these *CrWOXs*, we found that the number of introns varied from two to four (Fig. 3C). Analysis of cis-acting elements in the promoters of these WOXs allows prediction of which physiological processes they may respond to. Among them, we found that *CrWOX2*, *CrWOX8*, *CrWOX9*, *CrWOX10,* and *CrWOX14* have cis-acting regulatory elements related to the expression of meristematic tissues. In particular, there are two such elements in *CrWOX14*, which also contains cis-acting regulatory elements involved in the responsiveness of cofactors. These results all predict that *CrWOX14* may play an important function in promoting the regeneration of *C. rigescens*, as well as improving the transformation efficiency (Fig. 3D).

Regeneration and transformation system of *Carex rigescens*

We first established an efficient regeneration system for *C. rigescens.* High-quality yellow and compact embryogenic callus was obtained (Fig. 4A), and the callus tissue induction rate was 87%. *C. rigescens* callus tissues were infiltrated with *Agrobacterium tumefaciens* EHA105 with pGFPGUSPlus plasmid. Transient GUS staining was performed on the callus that had been co-cultured on filter paper for 2 d. It could be seen that parts of most of the healing tissues turned blue (Fig. 4B). The infested callus were continued in MS2 and screened for HygB resistance to kill callus that were not transformed. The surviving calli were transferred to the regeneration medium (MG) for shoot induction (Fig. 4C) and 1/2MS medium to develop roots (Fig. 4D). Transgenic seedlings were transferred into vermiculite and nutrient soil (1:1), and GUS staining of the transgenic seedlings showed that the part of the stem located close to the root was stained blue (Fig. 4F). DNA was extracted from the transgenic seedlings and tested by PCR using primers for HygB resistance genes, and a fragment of approximately 800 bp in length was obtained (Fig. 4G), with a transformation efficiency of 23%.

Meanwhile, in our experiments the pRI201-ON-GUS plasmid was also used for *C. rigescens* transformation, and transient GUS staining was performed on the callus that had completed the co-culture after the infestation (Figure S6), as well as staining the parts of the induced leaves. We found that large parts of the leaves were stained blue (Figure S7), which may be due to the enhancer of the plasmid that resulted in a high level of expression.

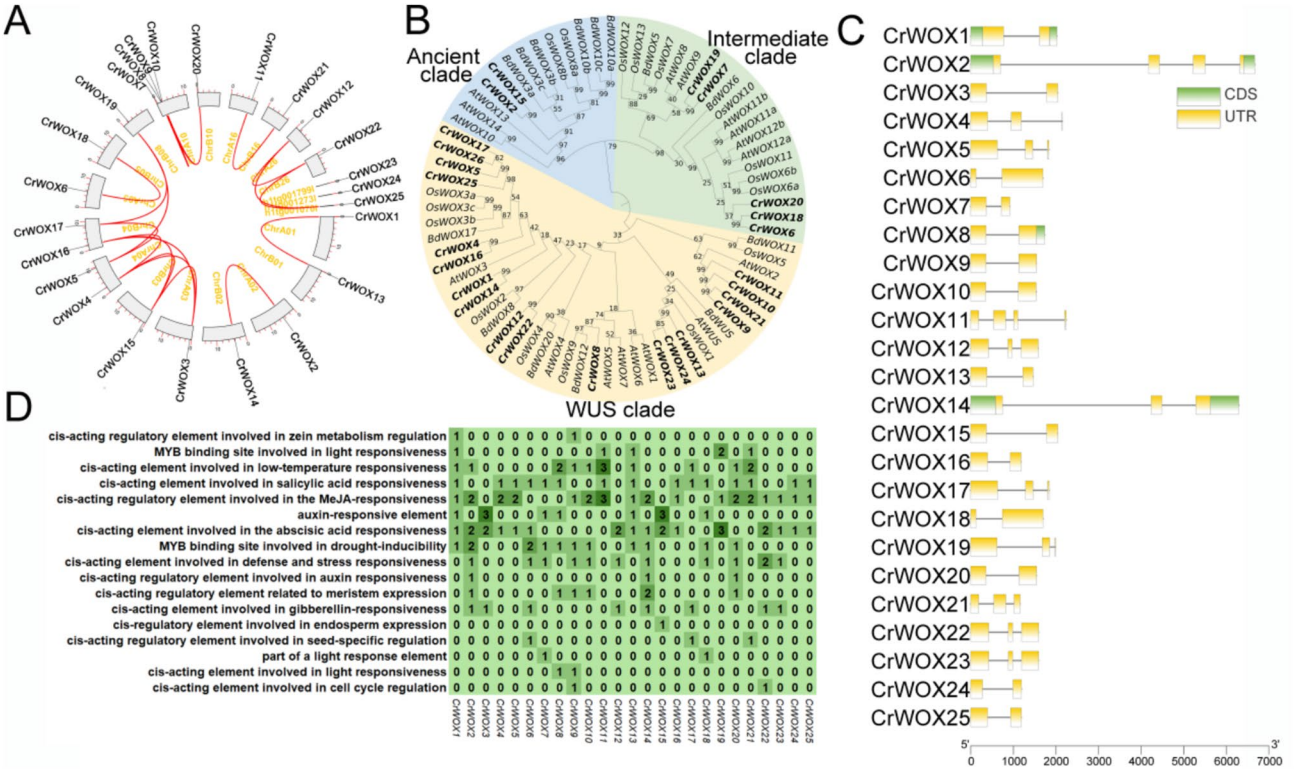

Fig. 3 **A** CrWOXs positions on the chromosomes of *C. rigescens*. **B** Classification of WOX. **C** WOX structure analysis of *C. rigescens*. **D** Cis-elements in the promoters of *CrWOX14*, the degree of green color and the numbers on the grid refer to the number of cis-elements of *CrWOX14*

Discussion

Carex rigescens (Franch) V. Krecz is highly tolerant to abiotic stresses such as cold, salt, drought, and high temperature (Ye et al. 2017; Hu et al. 2021). Due to its excellent adaptability to multiple abiotic stresses (especially salinity stress), low maintenance requirements, great potential as a turfgrass species in barren or arid soils, and outstanding ecological functions in remediation and nutrient absorption (Wu et al. 2024), *C. rigescens* has been highly valued for afforestation and ecological improvement in salinized urban and rural areas. Clarifying the chromosome number of *C. rigescens* is fundamental to understanding the karyotypic characteristics and the role of chromosome evolution in species diversity (Oliver et al. 2013). In this study, we obtained the ploidy as diploid and chromosome number as 60 of *C. rigescens* for the first time by combining chromosome visualization and flow cytometry. This is consistent with the chromosome number of some *Carex* species ,such as *C. stenophylla*, *C. diandra,* and *C. otrubae* (Rotreklova et al. 2011=). Almost all species of *Carex* are diploid. There is a wide variety of chromosome counts in the genus *Carex*, ranging from 18 to 108 (Wieclaw et al. 2020). The evolution of the genome and karyotype in the genus Carex was promoted by frequent chromosomal fusions, rare polyploidy, and common repetitive DNA proliferation/removal (Lipnerova et al. 2013).

We first analyzed the number of gene families in several species of *Carex* and *Arabidopsis thaliana* and found that *C. rigescens* has 2151 unique gene families. In constructing the phylogenetic tree, we found that the divergence of the genus *Carex* from the genus *Juncus* occurred at about 75 Mya, while the divergence of *C. rigescens* from *C. scoparia and C. cristatella* occurred at 7.7 Mya. We further clarified that chromosome doubling occurred only once in *C. rigescens* by WGD analysis. The chromosome doubling in *C. scoparia* and *C. littledalei* also had only one WGD event, while *C. cristatella* had two WGD events, which is consistent with what has been previously reported (Planta et al. 2022). LTR insertion events are often accompanied by genome size expansion and differentiation (Cai et al. 2018), and compared to other Carex, *C. rigescens* had a burst at 0.4 Mya compared to other Carex, while other Carex genera and Juncus genera were both later than *C. rigescens*, and we hypothesize that this may be due to the premature occurrence of WGD in *C. rigescens*.

The WOX (WUSCHEL-related homeobox) is a family of genes possessing a homologous heterodimeric structural domain (homeodomain, HD), and WUS was the first member of the *WOX* family of transcription factors to be discovered

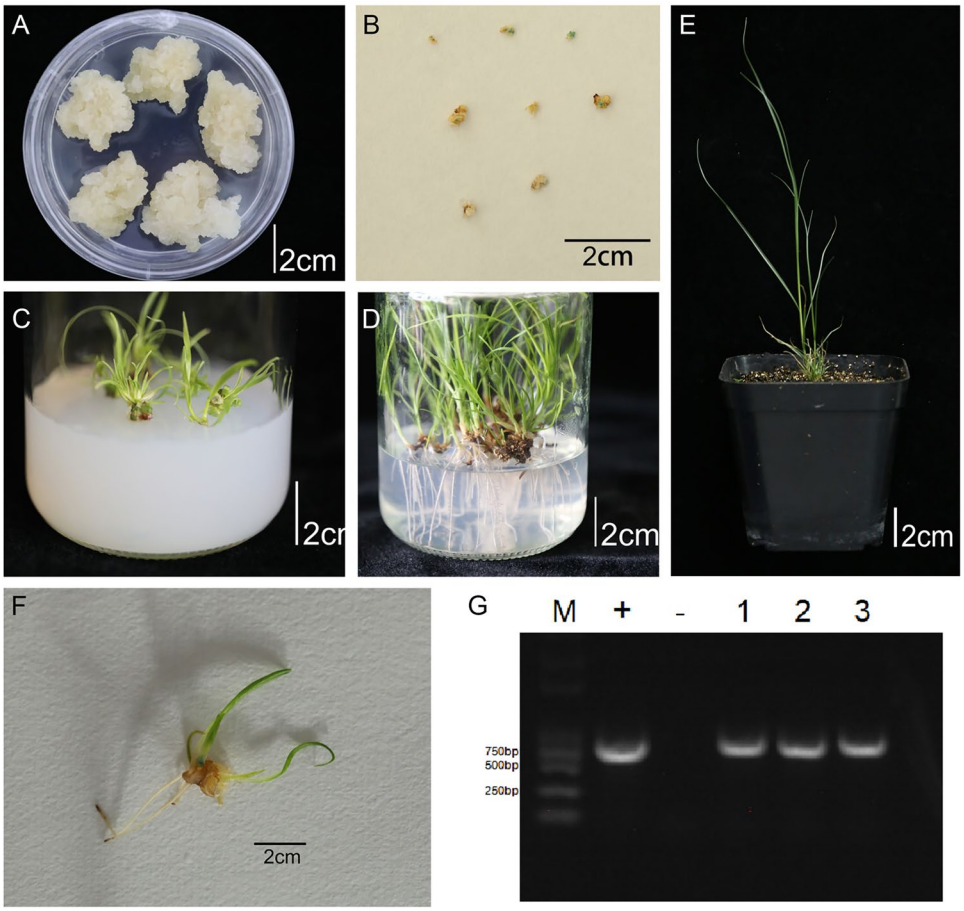

Fig. 4 Regeneration and transformation system of *Carex rigescens*. *A* An embryogenic callus of *Carex rigescens*. **B** Transient GUS staining of *Carex rigescens* callus. **C** Shoot developing of *Carex rigescens*. **D** Root development of *Carex rigescens*. **E** transgenic seedlings of *Carex rigescens*. **F** GUS staining of *Carex rigescens* transgenic seedlings. **G** PCR identification. M: Trans 2 K, + as plasmid positive control; —are non-transgenic seedlings (wild-type *Carex rigescens*), 1–3 are transgenic *Carex rigescens* plants), that is, PCR-positive plants

(Laux et al. 1996). Many WOX genes play important roles in many aspects of embryo development and polarity (Su et al. 2009), development of organs such as lateral buds (Lou et al. 2022), and abiotic stress (Lv et al. 2023). Because the *WUS* family has the above functions and does not have a large effect on plant phenotypes, increasing research has been focused on how to utilize *WUS/WOX* to improve plant regeneration and transgenic efficiency. For graminaceous plants, low regeneration efficiency is the main reason for low transgenic efficiency. Researchers first used AtWUS assistance during cotton regeneration and found that they were able to increase somatic embryogenesis to some extent (Bouchabké-Coussa et al. 2013). Subsequently, *TaWOX5* of wheat origin has been utilized to improve regeneration and transgenic efficiency in wheat and to break through the significance of genotype to wheat transgenics (Wang et al. 2022a). We found 25 family genes by analyzing the WOX family in *C. rigescens*, mainly on 17 chromosomes. Evolutionary analysis revealed that the WUS clade was the most distributed, and combined with promoter element analysis, *CrWOX14* was found to have multiple growth hormone and meristematic tissue-related regulatory elements, which was hypothesized to be a gene that may help to improve the regeneration and transformation efficiency of *C. rigescens*. This hypothesis needs to be further investigated, and in the future we will verify the gene function by constructing appropriate expression cassettes in order to be able to break the genotypic limitation of *C. rigescens*.

We first established the regeneration and transformation systems of *C. rigescens*, and both achieved high efficiency. Agrobacterium-mediated transformation of most species within the Cyperaceae family is challenging because of the resistance of these species to transformation, limited tissue culture regeneration, and genotype dependence (Shrawat and Loerz 2006; Mehrotra and Goyal 2012). Only a limited number of explants can be transformed and most transformation methods rely on immature embryos (Koetle et al. 2015). *C. rigescens* is highly fibrous, so among the types of explants used, only seeds induced callus tissues. Therefore, seeds are a more appropriate choice of explant for the induction of callus tissues in *C. rigescens*. The induced callus tissues were of various colors and morphologies. Generally speaking, embryonic callus tissues with brittle structure, vigorous growth, bright color, and faster proliferation were more likely to differentiate into seedlings (Zhou et al. 2021). Despite the low germination rate of *C. rigescens*, the rate of callus tissue induction and the percentage of embryonic callus tissue among all callus tissues were high.

This established *C. rigescens* transformation system provides a reliable technical platform for the genetic improvement of turfgrass varieties, especially for species with similar genetic backgrounds that are recalcitrant to conventional genetic manipulation. *CrUGT87A1*, a UDP-glycosyltransferase (UGT) gene derived from *Carex rigescens*, can enhance the salt tolerance of *Arabidopsis thaliana* by accumulating flavonoids and thus improving its antioxidant capacity (Zhang). In terms of turf architecture optimization, the manipulation of *CdCIPK29-A1*, a CIPK family gene derived from *Cynodon dactylon* L., via heterologous expression in *Arabidopsis thaliana*, revealed that this gene likely modulates stem growth angle and gravitropism by regulating starch metabolism in stem endodermal cells (Zhang and Liu 2025). In terms of turf quality optimization, the manipulation of TCP (TEOSINTE BRANCHED1 / CYCLOIDEA/PCF) family genes could regulate tiller development to form dense and compact turf canopies (Zhang and Liu 2018). Collectively, this transformation system bridges the gap between functional genomics research and practical turfgrass breeding, laying a foundation for the cultivation of high-performance, environment-friendly turfgrass varieties.

The pRI201-ON-GUS vector used in the transformation process is a vector for efficient expression of exogenous genes in monocotyledonous plant cells expressing a *GUS* reporter gene, which is mediated using an Agrobacterium rhizogenes (Sugio et al. 2010). The vector has a 5'-untranslated region (5'-UTR) of the rice alcohol dehydrogenase (ADH) gene as a transcriptional enhancer and an efficient terminator of the Arabidopsis heat shock protein (HSP) gene downstream of the 35S promoter. MCS2 is located downstream of the HSP terminator, where the expression cassette of the exogenous gene is inserted, so that multiple genes can be expressed simultaneously. The 5'-untranslated region (5'-UTR) of rice ADH can act as a translation enhancer in monocotyledonous plants such as rice. In this experiment, GUS transient staining of callus was carried out and counted to select the optimal conditions in the process of genetic transformation. This study demonstrates the basic feasibility of *the C. atrofusca* transformation system while definitive confirmation of stable integration (border junction PCR, copy-number analysis, T1 segregation) will be addressed in future work.

Conclusion

In conclusion, this study generated a high-quality chromosome-level genome assembly of *Carex rigescens* (2n = 60), anchoring 300 Mb of sequences to 30 chromosomes. The genome annotation identified 59,761 functionally annotated genes (91.28%) and 33.28% repetitive sequences, with evolutionary analyses revealing a WGD event and a recent LTR burst (~ 0.04 Mya). Additionally, we characterized the WOX gene family and established the first regeneration and transformation system for *C. rigescens*. These results fill the genomic resource gap for *Carex* species, provide a reference for comparative genomic studies of the genus, and lay a foundation for transgenic research and genetic improvement of *C. rigescens*.

Supplementary Information The online version contains supplementary material available at https://doi.org/10.1007/s00299-026-03796-8.

Author contributions L.W. and C.M. performed the experiments and analyzed the data. K.Z., C.W., and Y.W. analyzed part of the data and participated in the material preparation. L.W. and Y. S. wrote and revised the manuscript. Y.S. designed and funded the research. Y.L. and Q.H. designed part of the research and modified the language. All authors reviewed the results and approved the final version of the manuscript.

Funding This work was financially supported by the National Natural Science Foundation of China (Grant Nos. 32271763 and 32201465).

Data availability All data generated or analyzed in the present study are included in this article and in the additional information. The raw sequence data reported in this paper have been deposited in the Genome Sequence Archive (Genomics, Proteomics & Bioinformatics 2021) in the National Genomics Data Center (Nucleic Acids Res 2022), China National Center for Bioinformation/Bejing Institute of Genomics, Chinese Academy of Sciences (GSA:CRA017949) and are publicly accessible at https://ngdc.cncb.ac.cn/gsa.

Declarations

Conflict of interest The authors declare that they have no known competing financial interests or personal relationships that could have appeared to influence the work reported in this paper.

References

Beier S, Thiel T, Münch T et al (2017) MISA-web: a web server for microsatellite prediction. Bioinformatics 33:2583–2585. https://doi.org/10.1093/bioinformatics/btx198

Benson G (1999) Tandem repeats finder: a program to analyze DNA sequences. Nucleic Acids Res 27:573–580. https://doi.org/10.1093/nar/27.2.573

Bouchabké-Coussa O, Obellianne M, Linderme D et al (2013) Wuschel overexpression promotes somatic embryogenesis and induces organogenesis in cotton (*Gossypium hirsutum* L.) tissues cultured in vitro. Plant Cell Rep 32:675–686. https://doi.org/10.1007/s00299-013-1402-9

Buchfink B, Xie C, Huson DH (2015) Fast and sensitive protein alignment using DIAMOND. Nat Methods 12:59–60. https://doi.org/10.1038/nmeth.3176

Burton JN, Adey A, Patwardhan RP et al (2013) Chromosome-scale scaffolding of de novo genome assemblies based on chromatin interactions. Nat Biotechnol 31:1119–1125. https://doi.org/10.1038/nbt.2727

Cai X, Cui Y, Zhang L et al (2018) Hotspots of independent and multiple rounds of LTR-retrotransposon bursts in *Brassica* species. Hortic Plant J 4:165–174. https://doi.org/10.1016/j.hpj.2018.05.002

Cao Y, Zhao K, Xu J et al (2023) Genome balance and dosage effect drive allopolyploid formation in *Brassica*. Proc Natl Acad Sci U S A 120:e2217672120. https://doi.org/10.1073/pnas.2217672120

Chen S, Zhou Y, Chen Y, Gu J (2018) fastp: an ultra-fast all-in-one FASTQ preprocessor. Bioinformatics 34:i884–i890. https://doi.org/10.1093/bioinformatics/bty560

Chen C, Wu Y, Li J et al (2023) TBtools-II: A "one for all, all for one" bioinformatics platform for biological big-data mining. Mol Plant 16:1733–1742. https://doi.org/10.1016/j.molp.2023.09.010

Chen X, Hou Y, Cao Y et al (2024) A Comprehensive Identification and Expression Analysis of the WUSCHEL Homeobox-Containing Protein Family Reveals Their Special Role in Development and Abiotic Stress Response in *Zea mays* L. Int J Mol Sci 25:441. https://doi.org/10.3390/ijms25010441

Cheng H, Concepcion GT, Feng X et al (2021) Haplotype-resolved de novo assembly using phased assembly graphs with hifiasm. Nat Methods 18:170–175. https://doi.org/10.1038/s41592-020-01056-5

Ellinghaus D, Kurtz S, Willhoeft U (2008) LTRharvest, an efficient and flexible software for de novo detection of LTR retrotransposons. BMC Bioinformatics 9:18. https://doi.org/10.1186/1471-2105-9-18

Emms DM, Kelly S (2019) OrthoFinder: phylogenetic orthology inference for comparative genomics. Genome Biol 20:238. https://doi.org/10.1186/s13059-019-1832-y

Fambrini M, Usai G, Pugliesi C (2022) Induction of somatic embryogenesis in plants: different players and focus on WUSCHEL and WUS-RELATED HOMEOBOX (WOX) transcription factors. Int J Mol Sci 23:15950. https://doi.org/10.3390/ijms232415950

Flynn JM, Hubley R, Goubert C et al (2020) RepeatModeler2 for automated genomic discovery of transposable element families. Proc Natl Acad Sci U S A 117:9451–9457. https://doi.org/10.1073/pnas.1921046117

Friedman J, Barrett SCH (2009) The consequences of monoecy and protogyny for mating in wind-pollinated *Carex*. New Phytol 181:489–497. https://doi.org/10.1111/j.1469-8137.2008.02664.x

Galbraith DW, Lambert GM, Macas J, Dolezel J (2001) Analysis of nuclear DNA content and ploidy in higher plants. Curr Protoc Cytom Chapter 7:Unit 7.6. https://doi.org/10.1002/0471142956.cy0706s02

Griffiths-Jones S, Moxon S, Marshall M et al (2005) Rfam: annotating non-coding RNAs in complete genomes. Nucleic Acids Res 33:D121-124. https://doi.org/10.1093/nar/gki081

Haas BJ, Delcher AL, Mount SM (2003) Improving the *Arabidopsis* genome annotation using maximal transcript alignment assemblies. Nucleic Acids Res 31:5654–5666. https://doi.org/10.1093/nar/gkg770

Haas BJ, Salzberg SL, Zhu W et al (2008) Automated eukaryotic gene structure annotation using EVidenceModeler and the program to assemble spliced alignments. Genome Biol 9:R7. https://doi.org/10.1186/gb-2008-9-1-r7

Han MV, Thomas GWC, Lugo-Martinez J, Hahn MW (2013) Estimating gene gain and loss rates in the presence of error in genome assembly and annotation using CAFE 3. Mol Biol Evol 30:1987–1997. https://doi.org/10.1093/molbev/mst100

Hao Q, Zhang L, Yang Y et al (2019) Genome-wide analysis of the WOX gene family and function exploration of GmWOX18 in soybean. Plants 8:215. https://doi.org/10.3390/plants8070215

Hu Q, Cui H, Ma C et al (2021) Lipidomic metabolism associated with acetic acid priming-induced salt tolerance in *Carex rigescens*. Plant Physiol Biochem 167:665–677. https://doi.org/10.1016/j.plaphy.2021.08.045

Jha P, Ochatt SJ, Kumar V (2020) *WUSCHEL*: a master regulator in plant growth signaling. Plant Cell Rep 39:431–444. https://doi.org/10.1007/s00299-020-02511-5

Katoh K, Asimenos G, Toh H (2009) Multiple alignment of DNA sequences with MAFFT. Methods Mol Biol 537:39–64. https://doi.org/10.1007/978-1-59745-251-9_3

Keilwagen J, Wenk M, Erickson JL et al (2016) Using intron position conservation for homology-based gene prediction. Nucleic Acids Res 44:e89. https://doi.org/10.1093/nar/gkw092

Kim D, Langmead B, Salzberg SL (2015) HISAT: a fast spliced aligner with low memory requirements. Nat Methods 12:357–360. https://doi.org/10.1038/nmeth.3317

Koetle MJ, Finnie JF, Balazs E, Van Staden J (2015) A review on factors affecting the *Agrobacterium*-mediated genetic transformation in ornamental monocotyledonous geophytes. S Afr J Bot 98:37–44. https://doi.org/10.1016/j.sajb.2015.02.001

Korf I (2004) Gene finding in novel genomes. BMC Bioinformatics 5:59. https://doi.org/10.1186/1471-2105-5-59

Laux T, Mayer KF, Berger J, Jürgens G (1996) The WUSCHEL gene is required for shoot and floral meristem integrity in Arabidopsis. Development 122:87–96. https://doi.org/10.1242/dev.122.1.87

Lee L (1996) Turfgrass biotechnology. Plant Sci 115:1–8. https://doi.org/10.1016/0168-9452(96)04338-5

Lescot M, Déhais P, Thijs G (2002) PlantCARE, a database of plant cis-acting regulatory elements and a portal to tools for in silico analysis of promoter sequences. Nucleic Acids Res 30:325–327. https://doi.org/10.1093/nar/30.1.325

Li H, Durbin R (2009) Fast and accurate short read alignment with Burrows-Wheeler transform. Bioinformatics 25:1754–1760. https://doi.org/10.1093/bioinformatics/btp324

Lipnerova I, Bures P, Horova L, Smarda P (2013) Evolution of genome size in *Carex* (Cyperaceae) in relation to chromosome number and genomic base composition. Ann Bot 111:79–94. https://doi.org/10.1093/aob/mcs239

Longo C, Lickwar C, Hu Q et al (2006) Turf Grasses. Methods Mol Biol 344:83–95

Lou H, Huang Y, Wang W et al (2022) Overexpression of the AtWUSCHEL gene promotes somatic embryogenesis and lateral branch formation in birch (*Betula platyphylla* Suk.). Plant Cell, Tissue and Organ Culture (PCTOC) 150:371–383. https://doi.org/10.1007/s11240-022-02290-9

Lowe TM, Eddy SR (1997) tRNAscan-SE: a program for improved detection of transfer RNA genes in genomic sequence. Nucleic Acids Res 25:955–964. https://doi.org/10.1093/nar/25.5.955

Lv J, Feng Y, Jiang L et al (2023) Genome-wide identification of WOX family members in nine Rosaceae species and a functional analysis of *MdWOX13-1* in drought resistance. Plant Sci 328:111564. https://doi.org/10.1016/j.plantsci.2022.111564

Marçais G, Kingsford C (2011) A fast, lock-free approach for efficient parallel counting of occurrences of k-mers. Bioinformatics 27:764–770. https://doi.org/10.1093/bioinformatics/btr011

Mehrotra S, Goyal V (2012) *Agrobacterium*-mediated gene transfer in plants and biosafety considerations. Appl Biochem Biotechnol 168:1953–1975. https://doi.org/10.1007/s12010-012-9910-6

Mistry J, Chuguransky S, Williams L et al (2021) Pfam: The protein families database in 2021. Nucleic Acids Res 49:D412–D419. https://doi.org/10.1093/nar/gkaa913

Nawrocki EP, Eddy SR (2013) Infernal 1.1: 100-fold faster RNA homology searches. Bioinformatics 29:2933–2935. https://doi.org/10.1093/bioinformatics/btt509

Nguyen L-T, Schmidt HA, von Haeseler A, Minh BQ (2015) IQ-TREE: a fast and effective stochastic algorithm for estimating maximum-likelihood phylogenies. Mol Biol Evol 32:268–274. https://doi.org/10.1093/molbev/msu300

Oliver KR, McComb JA, Greene WK (2013) Transposable elements: powerful contributors to Angiosperm evolution and diversity. Genome Biol Evol 5:1886–1901. https://doi.org/10.1093/gbe/evt141

Oprea MI, Giosanu D, Vulpe M (2022) Decorative herbs, a green solution for urban arrangements. CTNS 11:356–364. https://doi.org/10.47068/ctns.2022.v11i21.039

Ou S, Jiang N (2018) LTR_retriever: a highly accurate and sensitive program for identification of long terminal repeat retrotransposons. Plant Physiol 176:1410–1422. https://doi.org/10.1104/pp.17.01310

Owen HR, Wengerd D, Miller AR (1991) Culture medium pH is influenced by basal medium, carbohydrate source, gelling agent, activated charcoal, and medium storage method. Plant Cell Rep 10:583–586. https://doi.org/10.1007/BF00232516

Pertea M, Pertea GM, Antonescu CM et al (2015) StringTie enables improved reconstruction of a transcriptome from RNA-seq reads. Nat Biotechnol 33:290–295. https://doi.org/10.1038/nbt.3122

Planta J, Liang Y-Y, Xin H et al (2022) Chromosome-scale genome assemblies and annotations for Poales species Carex cristatella, Carex scoparia, Juncus effusus, and Juncus inflexus. G3 Genes|genomes|genetics 12:jkac211. https://doi.org/10.1093/g3journal/jkac211

Qiao X, Zhang S, Paterson AH (2022) Pervasive genome duplications across the plant tree of life and their links to major evolutionary innovations and transitions. Comput Struct Biotechnol J 20:3248–3256. https://doi.org/10.1016/j.csbj.2022.06.026

Ranallo-Benavidez TR, Jaron KS, Schatz MC (2020) GenomeScope 2.0 and Smudgeplot for reference-free profiling of polyploid genomes. Nat Commun 11:1432. https://doi.org/10.1038/s41467-020-14998-3

Rao SSP, Huntley MH, Durand NC et al (2014) A 3D map of the human genome at kilobase resolution reveals principles of chromatin looping. Cell 159:1665–1680. https://doi.org/10.1016/j.cell.2014.11.021

Ren M, Chen Q, Li L (2005) Functional analysis of a reproductive organ predominant expressing promoter in cotton plants. Sci China C Life Sci 48:452–459. https://doi.org/10.1360/062004-71

Rice P, Longden I, Bleasby A (2000) EMBOSS: the European molecular biology open software suite. Trends Genet 16:276–277. https://doi.org/10.1016/s0168-9525(00)02024-2

Rogers SMD (2003) Tissue culture and wetland establishment of the freshwater monocots *Carex*, *Juncus*, *Scirpus*, and *Typha*. In Vitro Cell Dev Biol-Plant 39:1–5. https://doi.org/10.1079/IVP2002358

Rotreklova O, Bures P, Repka R et al (2011) Chromosome numbers of *Carex*. Preslia 83:25–58

Schütz W (1997) Are germination strategies important for the ability of cespitose wetland sedges (*Carex*) to grow in forests? Can J Bot 75:1692–1699. https://doi.org/10.1139/b97-883

Schütz W (1998) Seed dormancy cycles and germination phenologies in sedges (*Carex*) from various habitats. Wetlands 18:288–297. https://doi.org/10.1007/BF03161664

Schütz W (2000) Ecology of seed dormancy and germination in sedges (*Carex*). Perspect Plant Ecol Evol Syst 3:67–89. https://doi.org/10.1078/1433-8319-00005

Schütz W, Milberg P (1997) Seed dormancy in *Carex canescens*: regional differences and ecological consequences. Oikos 78:420–428. https://doi.org/10.2307/3545604

She R, Chu JS-C, Wang K et al (2009) GenBlastA: enabling BLAST to identify homologous gene sequences. Genome Res 19:143–149. https://doi.org/10.1101/gr.082081.108

Shrawat AK, Loerz H (2006) *Agrobacterium*-mediated transformation of cereals: a promising approach crossing barriers. Plant Biotechnol J 4:575–603. https://doi.org/10.1111/j.1467-7652.2006.00209.x

Simão FA, Waterhouse RM, Ioannidis P et al (2015) BUSCO: assessing genome assembly and annotation completeness with single-copy orthologs. Bioinformatics 31:3210–3212. https://doi.org/10.1093/bioinformatics/btv351

Stacey J, Isaac PG (1994) Isolation of DNA from plants. Methods Mol Biol 28:9–15. https://doi.org/10.1385/0-89603-254-x

Stanke M, Diekhans M, Baertsch R, Haussler D (2008) Using native and syntenically mapped cDNA alignments to improve de novo gene finding. Bioinformatics 24:637–644. https://doi.org/10.1093/bioinformatics/btn013

Su YH, Zhao XY, Liu YB et al (2009) Auxin-induced WUS expression is essential for embryonic stem cell renewal during somatic embryogenesis in Arabidopsis. Plant J 59:448–460. https://doi.org/10.1111/j.1365-313X.2009.03880.x

Su W, Xu M, Radani Y, Yang L (2023) Technological development and application of plant genetic transformation. Int J Mol Sci 24:10646. https://doi.org/10.3390/ijms241310646

Sugio T, Matsuura H, Matsui T et al (2010) Effect of the sequence context of the AUG initiation codon on the rate of translation in dicotyledonous and monocotyledonous plant cells. J Biosci Bioeng 109:170–173. https://doi.org/10.1016/j.jbiosc.2009.07.009

Tamura K, Stecher G, Kumar S (2021) MEGA11: molecular evolutionary genetics analysis version 11. Mol Biol Evol 38:3022–3027. https://doi.org/10.1093/molbev/msab120

Tang S, Lomsadze A, Borodovsky M (2015) Identification of protein coding regions in RNA transcripts. Nucleic Acids Res 43:e78. https://doi.org/10.1093/nar/gkv227

Tang Y, Li H, Guan Y et al (2020) Genome-wide identification of the Physic Nut WUSCHEL-related homeobox gene family and functional analysis of the abiotic stress responsive Gene*JcWOX5*. Front Genet 11:670. https://doi.org/10.3389/fgene.2020.00670

Tarailo-Graovac M, Chen N (2009) Using RepeatMasker to identify repetitive elements in genomic sequences. Curr Protoc Bioinformatics Chapter 4:4.10.1-4.10.14. https://doi.org/10.1002/0471250953.bi0410s25

Vickers CE, Schenk PM, Li D et al (2007) pGFPGUSPlus, a new binary vector for gene expression studies and optimising transformation systems in plants. Biotechnol Lett 29:1793–1796. https://doi.org/10.1007/s10529-007-9467-6

Wan M (2001) A new lawn plant resource:genus Carex L. Pratacult Sci 18(2):43–45

Wang Y, Tang H, Debarry JD et al (2012) MCScanX: a toolkit for detection and evolutionary analysis of gene synteny and collinearity. Nucleic Acids Res 40:e49. https://doi.org/10.1093/nar/gkr1293

Wang L-Q, Wen S-S, Wang R et al (2021) PagWOX11/12a activates PagCYP736A12 gene that facilitates salt tolerance in poplar. Plant Biotechnol J 19:2249–2260. https://doi.org/10.1111/pbi.13653

Wang K, Shi L, Liang X et al (2022a) The gene TaWOX5 overcomes genotype dependency in wheat genetic transformation. Nat Plants 8:110–117. https://doi.org/10.1038/s41477-021-01085-8

Wang Y, He S, Long Y et al (2022b) Genetic variations in ZmSAUR15 contribute to the formation of immature embryo-derived

embryonic calluses in maize. Plant J 109:980–991. https://doi.org/10.1111/tpj.15609
Wieclaw H, Kalinka A, Koopman J (2020) Chromosome numbers of *Carex* (Cyperaceae) and their taxonomic implications. PLoS ONE 15:e0228353. https://doi.org/10.1371/journal.pone.0228353
Willoughby AC, Nimchuk ZL (2021) WOX going on: CLE peptides in plant development. Curr Opin Plant Biol 63:102056. https://doi.org/10.1016/j.pbi.2021.102056
Wingett SW, Ewels P, Furlan-Magaril M et al (2015) HiCUP: pipeline for mapping and processing Hi-C data. F1000Research 4:1310
Wu Y, Zhu K, Wang C et al (2024) Comparative metabolome and transcriptome analyses reveal molecular mechanisms involved in the responses of two *Carex rigescens* varieties to salt stress. Plants Basel 13:2984. https://doi.org/10.3390/plants13212984
Xu Z, Wang H (2007) LTR_FINDER: an efficient tool for the prediction of full-length LTR retrotransposons. Nucleic Acids Res 35:W265-268. https://doi.org/10.1093/nar/gkm286
Yadav S, Kalwan G, Meena S et al (2023) Unravelling the due importance of pseudogenes and their resurrection in plants. Plant Physiol Biochem 203:108062. https://doi.org/10.1016/j.plaphy.2023.108062
Ye YR, Wang WL, Zheng CS et al (2017) Evaluation of cold resistance of four wild Carex speices. Ying Yong Sheng Tai Xue Bao 28:89–95
Zhang B, Liu J (2018) Molecular cloning and sequence variance analysis of the *TEOSINTE BRANCHED1* (*TB1*) gene in bermudagrass [*Cynodon dactylon* (L.) Pers]. J Plant Physiol 229:142–150. https://doi.org/10.1016/j.jplph.2018.07.008
Zhang B, Liu J (2025) Genome-wide analysis of CBL and CIPK gene families in bermudagrass reveals the CdCIPK29-A1 as a stem growth angle regulator. Plant Cell Rep 44:68. https://doi.org/10.1007/s00299-025-03457-2
Zhang K, Sun Y, Li M, Long R (2021) *CrUGT87A1*, a UDP-sugar glycosyltransferases (UGTs) gene from *Carex rigescens*, increases salt tolerance by accumulating flavonoids for antioxidation in *Arabidopsis thaliana*. Plant Physiol Biochem 159:28–36. https://doi.org/10.1016/j.plaphy.2020.12.006
Zhou C, Wang S, Zhou H et al (2021) Transcriptome sequencing analysis of sorghum callus with various regeneration capacities. Planta 254:33. https://doi.org/10.1007/s00425-021-03683-4
Zwaenepoel A, Van de Peer Y (2019) wgd-simple command line tools for the analysis of ancient whole-genome duplications. Bioinformatics 35:2153–2155. https://doi.org/10.1093/bioinformatics/bty915